

Assessment of Urban Heat Islands in Brazil based on MODIS remote sensing data

Felipe Ferreira Monteiro ^{a,*}, Weber Andrade Gonçalves ^a,
 Lara de Melo Barbosa Andrade ^a, Lourdes Milagros Mendoza Villavicencio ^a,
 Cássia Monalisa dos Santos Silva ^b

^a Federal University of Rio Grande do Norte, University Campus Lagoa Nova, Natal, Rio Grande do Norte 59078-970, Brazil

^b State University of Goiás, Niquelândia, Goias 76420-000, Brazil

ARTICLE INFO

Keywords:

Urban climate
 Urban energy balance
 Thermal remote sensing
 Albedo

ABSTRACT

Estimates indicate that by 2050, 70% of the world's population will live in urban areas, expanding the total built-up space and density of those areas. The urban heat island (UHI) phenomenon causes increased temperatures in urban areas compared to outlying regions. It is considered one of the main anthropogenic climate modifications and is directly linked to land-use patterns. The objective of this study was to analyze the presence of the UHI effect, diurnal and nocturnal, in the dry season in 21 Brazilian metropolitan areas from 2000 to 2016. Surface temperature, mean albedo, and normalized difference vegetation index (NDVI) values generated by the MODIS sensor (Moderate-resolution Imaging Spectroradiometer) were used. The results obtained showed substantial differences between diurnal and nocturnal UHI effects. Manaus, Porto Alegre, Belém, and Recife presented the highest values of diurnal UHI, whereas Curitiba, Brasília, São Paulo, and Rio de Janeiro showed higher heat island effects at night. The results are an alert to policymakers of the need to rethink land occupation regulations and also give support to actions to mitigate the phenomenon.

1. Introduction

The urbanization process in Brazil, as in other countries, has caused large changes in the natural environment. Changes in surface characteristics directly influence energy flows. The transformations resulting from urbanization also influence the surface energy balance, which in turn is reflected in atmospheric properties and creates a particular climatic condition in urban areas known as urban climate (Oke, 1987).

As a consequence of the high built density, verticalization, ground waterproofing and other peculiarities of urban surfaces, there is a surface energy imbalance, generating a local disturbance in the regional climate called the urban heat island (UHI) effect, classified as one of the main anthropogenic influences on the global climate (Oke, 1987; Oke et al., 1992; Dwivedi and Khire, 2018). According to Mills (2008), the UHI effect occurs when there is an increase of air and surface temperature in urban areas compared to the surrounding rural areas. The subject has been widely reported and investigated in cities of different sizes around the world (Arnfield, 2003; Zhang et al., 2012; Zhou et al., 2017; Rizwan et al., 2008; Stewart, 2011).

* Corresponding author.

E-mail address: felipefmonteiro@gmail.com (F.F. Monteiro).

The quantification and monitoring of UHI allow policymakers to assess risks and seek ways to mitigate this phenomenon. However, the identification and analysis of UHI faces a conceptual issue. The lack of clear and consistent definition of urban and rural areas makes it difficult to compare UHI studies in different areas of the world (Stewart and Oke, 2012).

Constantinescu et al. (2016) observed the impacts caused by the presence of UHI, in particular the various health risks, including increased mortality, due to thermal stress (Anderson and Bell, 2009; Zhou et al., 2015; Zhou et al., 2015; Yang et al., 2017; Inouye, 2015; McDonnell and MacGregor-Fors, 2016; Lee et al., 2015). The impacts on the health of people due to continuous exposure to high temperatures and low humidity include discomfort, dehydration, sunstroke and cerebrovascular diseases (Martínez Navarro et al., 2004; Laforteza et al., 2009; Sachindra et al., 2016; Akbari and Matthews, 2012). Other consequences are economic, due to the increase in energy demand for cooling of buildings in densely populated areas (Rizwan et al., 2008; Kolokotsa et al., 2018).

Many studies have used *in situ* measurements collected by meteorological stations, but the definition of only one of a few collection points does not reflect the great heterogeneity of urban surfaces (Buyantuyev and Wu, 2010; Cadenasso et al., 2007). Due to this drawback, the use of orbital data is of great importance to study the phenomenon. Lombardo (1985) was the pioneer among researchers who used remote sensing databases in Brazil to identify warming and its relationships with different land-uses. The results showed that industrial regions and areas with less vegetation cover within the urban core of São Paulo were associated with the UHI phenomenon. Since the first efforts in Brazil to analyze the UHI effect, many other methods and sensors have been applied, such as Landsat TIRS (Thermal Infrared Sensor); CBERS IRS; and Moderate Resolution Imaging Spectroradiometer (MODIS) of the Aqua and Terra satellites. Some studies have used only one satellite overpass to obtain temperature anomalies and analyze a city, such as Souza et al. (2009), Macedo Neto et al. (2011), Lemos (2011), Naccarato et al. (2003) and Mashiki and Campos (2013), for the cities of São Paulo, Petrolina, Curitiba, Goiânia, and Botucatu, respectively. The authors observed that surface temperature anomalies are associated with high the density of buildings and less ground plant cover.

Other studies have used more than one satellite overpass to analyze the land-use dynamics in association with the surface temperature, such as for the cities of Fortaleza (Silva et al., 2011), Goiânia (Sousa and Ferreira, 2012) Piracicaba (Polizel, 2009; Coltri et al., 2009), Recife (Santos, 2011), Rio de Janeiro (Fuckner et al., 2009; Kazay et al., 2011) and São Paulo (Fuckner et al., 2009). Some of these studies were developed with a temporal resolution of daily differences between scenarios. Thus, the data might have been affected by meteorological conditions, like cloud cover, increasing possible inaccuracies related to data acquisition.

For daily monitoring studies, MODIS is the sensor used most often. It provides a large number of terrestrial surface products, which undergo regular calibration and validation control (Du et al., 2016; Li et al., 2017). Among the studies that have used MODIS data, Corrêa (2011) used surface temperatures and the normalized difference vegetation index (NDVI) values to identify temperature anomalies and urban climate changes for the city of Belém. The study found some hotspots that were correlated with lower NDVI values, in addition to identifying changes in the position of hotspots in the metropolitan region of Belém. Souza et al. (2016) used MODIS data in combination with mesoscale numerical modeling (Brazilian Regional Atmospheric Modeling System - BRAMS) to study UHI for Belém and Manaus, two cities in the Amazon. The authors observed great differences in surface temperature, nearly 3 °C, between the urban areas and their surroundings, as well as lower humidity in urban areas.

Campelo et al. (2018) used data from the MODIS sensor to assess daily and nightly urban temperatures between 2000 and 2016 in the cities of Natal and Fortaleza, in northeastern Brazil. The presence of the UHI effect was observed in both cities, with the largest being found in Fortaleza, of around 4 °C. The authors commented that the change in vegetation cover in the border areas increases the NDVI differentials, increasing the intensity of UHI temperature rise in cities. However, the study did not present more detailed evaluation of the behavior of surface temperature.

MODIS images were also used to identify UHI in the South and Southeast regions of Brazil. Sena et al. (2014) identified the presence of UHI in the city of Rio de Janeiro. The authors highlighted changes surface temperature for all seasons, finding differentials of up to 10 °C between the urbanized core and the urban edge in summer. In the metropolitan region of São Paulo, Naccarato et al. (2003) and Bourscheidt et al. (2016) identified the presence of the phenomenon associated with the occurrence of lightning. For the metropolitan region of Curitiba, Lunardon (2017) evaluated the behavior of urban temperatures and identified that regions with higher values were associated with greater incidence of dengue fever cases.

The foregoing reveals that studies of UHI have been carried out in all five macro-regions in Brazil (South, Southeast, Midwest, Northeast, and North). These previous studies have mainly focused on the analysis of UHI in single cities, or at most two. Besides this, little attention has been given to UHI studies of Brazil as a whole. Thus, a systematic study of factors associated with the intensity of UHIs in the major Brazilian metropolises is important. Therefore, this study aims to identify and analyze the UHI phenomenon and its changes over the past few years related to potential influential factors such as urban density, population volume, surface albedo and vegetation cover index.

More specifically, this study analyzes the day and night UHI effects in 21 different metropolitan regions of Brazil, from 2000 to 2016. Besides, it describes temporal trends and evaluates the differences and similarities between metropolises in relation to UHI, vegetation, surface albedo, and population factors.

2. Materials and methods

2.1. Study area

All Brazilian metropolises were analyzed, composed of the metropolitan regions of the state capitals with population over 750,000 inhabitants, totaling 21 metropolises distributed throughout the country (Fig. 1).

Urban and residential densities are important components to study the UHI phenomenon (Grimmond, 2007; Deilami et al., 2018).

In this sense, Table 1 presents the demographic aspects of the studied metropolises. Among them, 17 had more than 1 million inhabitants in 2010, mostly located on the east coast. The city of Manaus also stands out, with the highest household density, while Belém and Recife have the highest urban densities among the metropolises (Table 1).

Considering that Brazilian metropolises are located in different latitude belts (Fig. 1), each of these places is affected by specific environmental aspects, such as total hours of insolation and active meteorological systems, which modulate wet and dry periods.

2.2. Data

For this study, we used different products derived from images collected by the MODIS sensor aboard the TERRA satellite, between 2000 and 2016. The TERRA satellite collects information from the surface in 36 bands, varying from visible to infrared. This satellite has an almost polar synchronous solar orbit, passing everywhere on Earth twice a day, at approximately 10:30 LT and 22:30 LT.

The MODIS thermal infrared sensors (TIR) measure radiation from the top of the atmosphere (TOA), from which brightness temperatures can be derived using Planck's law. These brightness temperatures are different from the real land surface temperatures (LST), with a difference between 1 and 5 K, due to the satellite's non-vertical viewing angle, urban geometry, variable surface emissivity, and various atmospheric effects (Dousset and Gourmelon, 2003). To remove these effects and estimate the LST from space, a method called MODIS LST day-night was designed to take advantage of the unique capacity of the MODIS instrument (Wan, 2014).

The day-night MODIS LST method uses TIR data pairs in seven MODIS bands for the simultaneous recovery of surface temperatures and mean band emissivity in bands 20, 22, 23, 29, and 31–33 without knowing the water vapor profiles and atmospheric temperature with high precision (Wan et al., 2004). Besides this, to generate more regionally representative urban temperature estimates, the three-dimensional roughness of urban surfaces was considered, which depends on the scale of the satellite images (Voogt and Oke, 2003).

Thus, in the present study, we employed MODIS global land surface temperature (LST) level 3 (MOD11A2) data, which are composed of the mean values of clear-sky LSTs over a period of 8 consecutive days with a spatial resolution of 1 km² (Wan et al., 2004; Wan, 2014). All told, we used 1550 images (775 daytime and 775 nighttime). Cloud-covered pixels and other atmospheric disturbances were excluded for better information quality. The surface temperature is an important parameter for urban climate studies, since it directly influences human comfort, modulating the air temperature in the lower layers of the atmosphere and affecting the exchange of energy (Voogt and Oke, 2003).

The degree of vegetation vigor is usually measured by different indexes based on orbital data (Jesen, 2009). The dimensionless measures with higher values mean that the land is covered by healthy vegetation, which plays an important role in urban areas to improve comfort due to shade and capture of radiation (Campelo et al., 2018).

In this study, we adopted the normalized difference vegetation index (NDVI), a measure that is highly correlated with vegetation density (Carlson and Ripley, 1997). NDVI data are available in a way that allows consistent spatial and temporal comparisons of vegetation conditions. For its determination, MODIS uses blue, red, and near-infrared reflectance, centered at 470 nm, 648 nm, and 848 nm, respectively. The MODIS Terra, MOD13A2 product, version 006, was used in this study. This product provides a mean value of

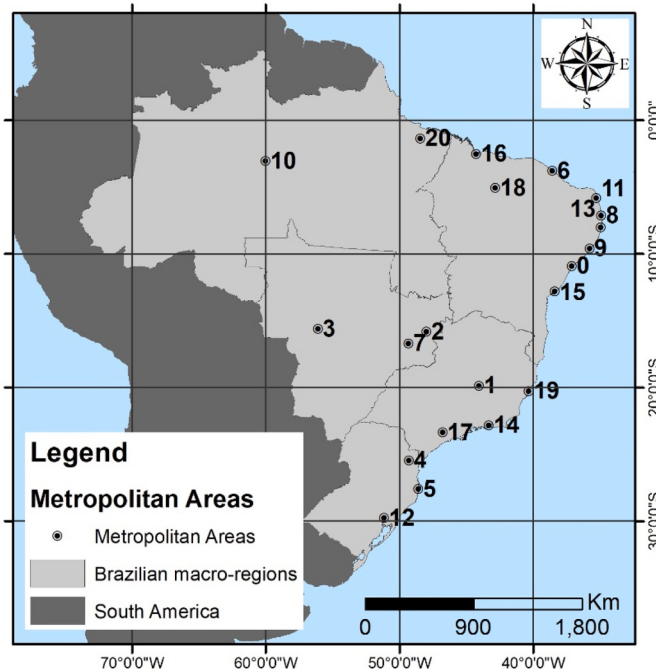


Fig. 1. Spatial distribution of the 21 metropolises used in the present study. The name of each is identified by its number in Table 1.

Table 1

Total population, urban, and household density of the metropolises studied.

	Metropolitan Area	Total Population (2010 Census)	Urban Population Density	Urban Household Density
			(Persons/Hectare)	(Dwellings/Hectare)
0	Aracaju	926,399	28.71	8.36
1	Belo Horizonte	4,728,059	23.08	7.14
2	Brasília	3,380,644	17.82	5.32
3	Cuiabá	803,694	17.85	5.36
4	Curitiba	3,054,076	22.23	7.08
5	Florianópolis	883,808	11.33	3.82
6	Fortaleza	3,327,021	26.00	7.46
7	Goiânia	2,042,828	19.11	6.05
8	João Pessoa	1,050,872	36.90	10.82
9	Maceió	1,115,485	41.20	12.05
10	Manaus	1,802,014	39.04	20.50
11	Natal	1,187,899	26.64	7.81
12	Porto Alegre	3,662,262	15.95	5.42
13	Recife	3,741,904	43.08	13.06
14	Rio de Janeiro	11,946,398	25.05	8.07
15	Salvador	3,440,462	27.86	8.86
16	São Luiz	1,265,603	21.05	5.70
17	São Paulo	19,613,759	18.07	5.52
18	Teresina	986,831	25.77	7.02
19	Vitória	1,582,418	25.31	8.04
20	Belém	2,025,276	45.06	11.93

Source: Demographic Census (IBGE, 2016).

the NDVI for 16 consecutive days, with spatial resolution of 1 km^2), for a total of 338 images for each metropolitan area. Pixels with the presence of cloud cover and other atmospheric noises were also excluded.

The materials used in the urban environment have an important role in the thermal balance. The impact on the urban atmosphere depends on how they absorb and reflect the incident radiation. The dissipated thermal energy heats the air near the surface and affects the urban temperature (Taha, 1997; Kruger, 2016). The data provided by the MCD43A3 product, version 006, were used. The product provides daily information based on the average of 16 consecutive days of surface reflection, centered on the ninth day of the series. The spatial resolution of the product is 500 m^2 , in which the pixels with the presence of cloud cover and other atmospheric disturbances were excluded for higher data quality. Due to the daily coverage of the product, a total of 6150 images were used.

The values are separated into two factors, the directional hemispheric reflectance, called the black-sky albedo, which captures the direct reflection of incident light without the presence of diffusion, and the bi-hemispheric reflectance, called white-sky albedo, which captures diffuse reflection without considering the direct incidence of solar radiation (Schaaf, 2015). For this study, the daily average albedo was used, albedo black-sky and white-sky were calculated as daily averages to derive general surface albedo, since they allowed obtaining results without the need to collect in the field or model estimates of aerosol concentration parameters and water vapor column or other parameters. We wound up obtaining results with a very low margin of error, on the order of 0.009, as discussed by Su et al. (2007).

To separate urban and rural areas, the MODIS Land Cover Type Climate Modeling Grid (CMG), product MCD12Q1, was used

Table 2

Landcover Type 1: International Geosphere-Biosphere Program (IGBP) global vegetation classification scheme.

Class	IGBP(Type 1) land cover index
0	Water
1	Evergreen needleleaf forest
2	Evergreen broadleaf forest
3	Deciduous needleleaf forest
4	Deciduous broadleaf forest
5	Mixed forest
6	Closed shrublands
7	Open shrublands
8	Woody savannas
9	Savannas
10	Grasslands
11	Permanent wetlands
12	Croplands
13	Urban and built-up areas
14	Croplands/natural vegetation mosaics
15	Snow and ice
16	Barren or sparsely vegetated land

(Strahler et al., 1999; Schwarz et al., 2011), which has a spatial resolution of 500 m, and classifies the Earth's surface according to the International Geosphere-Biosphere Project (IGBP). The land cover classification scheme identifies a total of 17 classes (Table 2), which include 11 classes of natural vegetation, 3 classes of mosaic uses and 3 classes of non-vegetated land. In this categorization, the urban category was obtained from the observations of MODIS version 4, in line with Friedl et al. (2002). Based on the official urban limits of each of the 21 metropolitan areas studied, all pixels of the urban category inserted in the respective boundaries were defined as the urban core of the metropolitan area.

Another important data source used in this study was the climatological normals (INMET, 2018) of each metropolitan region, obtained by the monthly average of 30 years of records, from 1981 to 2010. These data were used to determine the dry period for each of the metropolitan regions evaluated. The method for determining the dry season is described in the next section.

2.3. Methods

The UHI effect is greater in certain conditions, such as during periods of low wind speed with few or no clouds, as observed by various authors (Oke, 1982; Morris et al., 2001; Voogt and Oke, 2003; Wienert and Kuttler, 2005). In addition, such conditions, especially lower cloudiness, facilitate the identification of UHI by remote sensing. Considering this premise, the dry season of each metropolitan area was determined as the months in which the monthly accumulated precipitation was below the annual average minus the climatological standard deviation. Only the images captured during the dry season of each metropolitan area were used to determine the heat island effect and obtain the values of NDVI and surface albedo.

The intensity of the UHI effect (during the day and night) was calculated by the difference between the mean temperature of the pixels present in the metropolitan area (T_{urban}) and the pixels of the metropolitan edge (T_{edge}). This definition, denoted by Eq. (1), is an approximation of the traditional method in which two weather stations are compared, one urban and the other rural, typically adopted in UHI analysis. The border region is defined as the area beyond a certain distance from the urban boundary, as shown in Fig. 2.

$$\text{UHI} = T_{\text{urban}} - T_{\text{edge}} \quad (1)$$

According to Schwarz et al. (2011), determining an ideal value for the urban edge is a difficult task due to the variability of the different study sites. In this sense, different edge dimensions were verified and the results showed no significant changes in mean temperature values. For this, some urban edge dimensions were tested as 2 km, 3 km, 4 km, and 5 km. No significative statistical

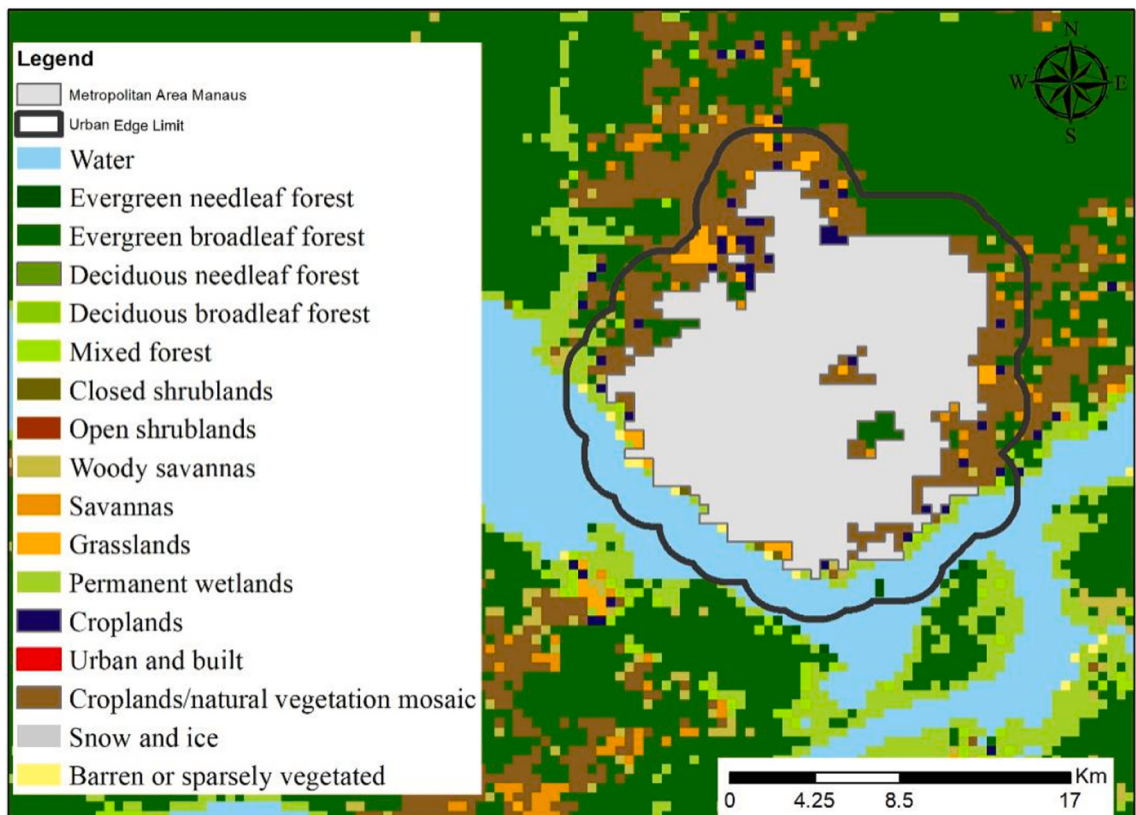


Fig. 2. Example of delimitation of the areas of the core (gray area) and urban edge limit (black line) for the metropolitan area of Manaus, with the land-use surface according to the IGBP classification.

difference was observed between the dimensions. Thus, in line with the recommendations of other studies (Peng et al., 2012; Clinton and Gong, 2013; Du et al., 2016; Zhao et al., 2016), we chose the value of 2000 m away from the urban area. This choice prevented overlapping data from different metropolises. Fig. 2 contains an example of the selection of urban and edge regions in metropolitan areas of this study. This example is the metropolitan area of Manaus, which is located in the heart of the Amazon Forest. Land cover types from classification of IGBP are also shown.

It is important to mention that the spatial resolution of the land cover product (MCD12Q1) and the surface temperature product (MOD11A2) are different. The first one has a pixel of 500 m² and the second 1 km². To deal with this issue without losing any information from the data, the calculation of T_{edge} and T_{urban} considered the pixels in the surface temperature product in which all pixels were completely within or outside the urban areas, respectively, totaling four pixels from the land cover product. The same procedure was performed for the NDVI (MOD13A2) and albedo (MCD43A3) products.

The calculation of the UHI (Eq. 1) allows rapid identification of the phenomenon because it is assumed that the heating of the urban and rural surface occurs in the same proportion (Hausfather et al., 2013). The t-statistic of paired means was applied at a confidence level of 95% to assure statistical significance between the temperature of the urban and the border areas.

The variation of albedo and NDVI values between the urban core and its edge, called Δ_{Albedo} and Δ_{NDVI}, respectively, were calculated according to the equations below:

$$\Delta_{\text{Albedo}} = \text{ALBEDO}_{\text{urban}} - \text{ALBEDO}_{\text{edge}} \quad (2)$$

$$\Delta_{\text{NDVI}} = \text{NDVI}_{\text{urban}} - \text{NDVI}_{\text{border}} \quad (3)$$

Where ALBEDO_{urban} and ALBEDO_{edge} are the mean albedo values of the urban and edge areas, respectively, and NDVI_{urban} and NDVI_{edge} follow the same pattern.

To determine the existence of trends in UHI intensity values over time, the Mann-Kendall (MK) nonparametric statistical test was applied, which predicts the trend of the series but does not provide an estimate of the value. Two hypotheses were tested using the MK test: the null hypothesis, H₀, that there is no trend in the time series; and the alternative hypothesis, H_a, that there is a statistically significant trend in the series, for a given α significance level. Kendall's τ is defined as the actual rating score of correlation divided by the maximum probable score. The MK coefficient (Mann, 1945; Kendall, 1975) is calculated as:

$$\sum_{k=1}^{n-1} \sum_{j=k+1}^n \text{sign}(x_j - x_k) \quad (4)$$

where n is the number of observation values in the series; x₁, x₂, ... x_n represent n data points where x_j represents the data point at

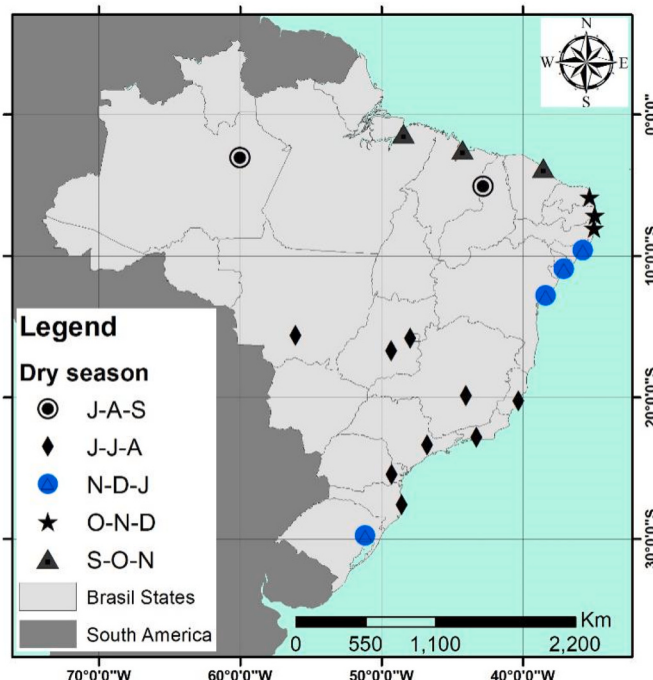


Fig. 3. Classification of the dry season of the 21 metropolises studied in Brazil. The initials JAS, JJA, NDJ, OND, and SOD represent the months of July-August-September, June-July-August, November-December-January, October-November-December, and September-October-November, respectively.

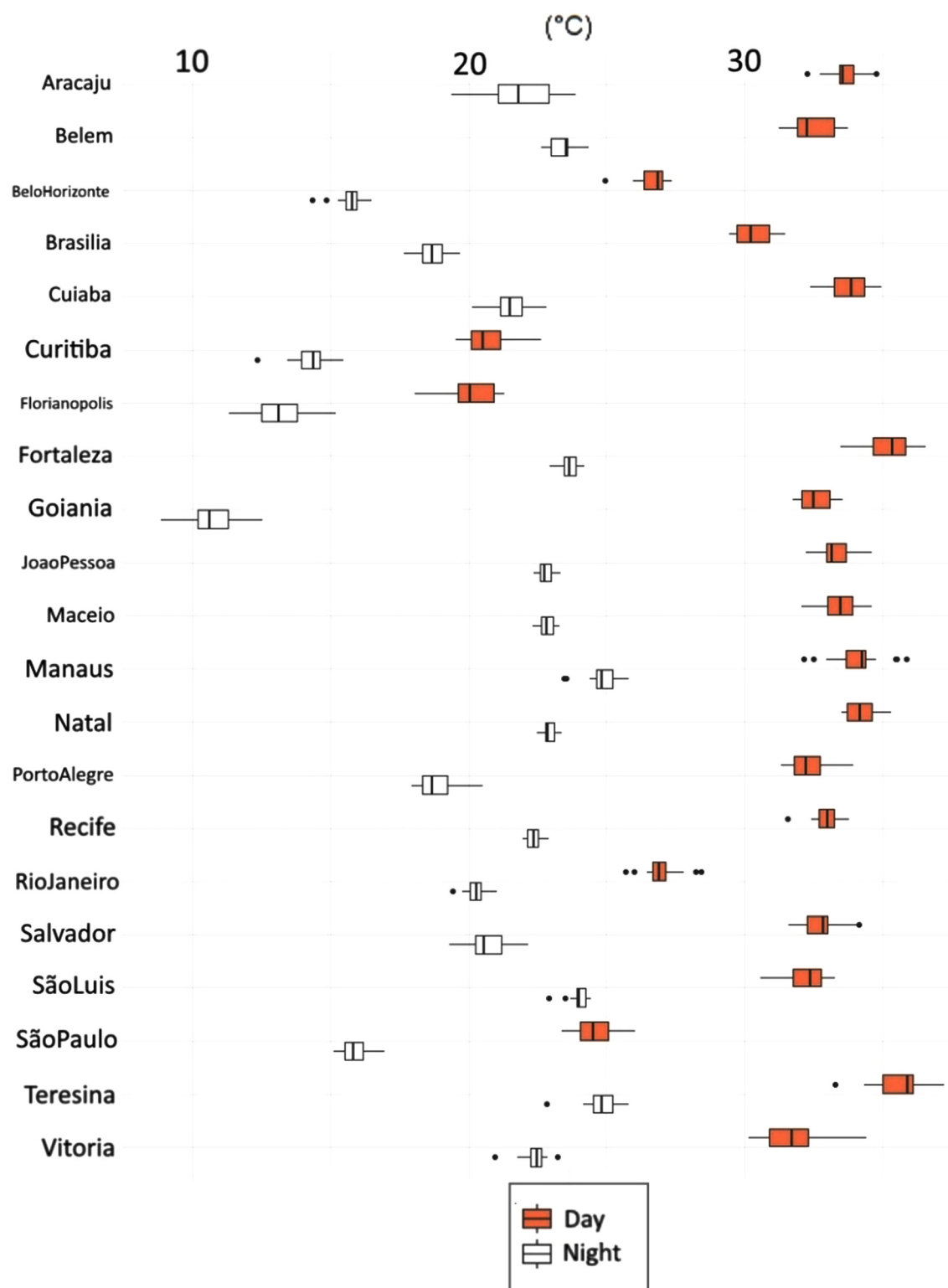


Fig. 4. Boxplot of mean day and night surface temperatures in the dry season for the urban surface during the analyzed period.

time j ; and sign $(x_j - x_k)$ is the sign function, in turn:

$$\text{sign}(x_j - x_k) = \begin{cases} 1, & x_j > x_k \\ 0, & x_j = x_k \\ -1, & x_j < x_k \end{cases} \quad (5)$$

A high positive value of S indicates an increasing trend while a low negative value is an indicator of a decreasing trend. To obtain this estimate, the Theil-Sen (TS) estimator was applied to estimate the trend of values. This method has the advantage that it is only minimally influenced by the effects of abnormal or extreme records in the time series (Yavasli, 2017).

In this study, we evaluated a historical series of 20 years of UHI data during the dry period of each metropolitan area. Thus, for a better understanding of the results, we present the trends by decades, as indicated by Yao et al. (2015) and Lee et al. (2020).

After the analysis of the UHI intensities, cluster analysis (CA) was applied to the data to understand the differences and similarities of the phenomenon in the 21 metropolises studied. After selecting a distance measure to quantify dissimilarity or similarity between the elements, the next step in CA is to choose a method or grouping criterion to determine the association of the different data pairs. For this study, Ward's hierarchical method was used (Wilks, 2011). The CA was applied to the UHI values during the daytime and nighttime, respectively, and the albedo and NDVI values were analyzed to understand their influence on the intensity of the UHI effect.

3. Results

3.1. Evaluation of the dry season

The dry season of each metropolitan area had great variability during each year (Fig. 3). However, nine of the evaluated metropolises had dry season in the austral winter. These metropolitan areas are located in the South and Midwest regions of Brazil, where during this season there are frequent incursions of cold and dry air masses (Cavalcanti and Kousky, 2003).

For the metropolises located in the eastern part of Northeast Brazil (NEB), the dry period is during the months November-December-January and October-November-December. The rainy season in the eastern NEB is primarily in the austral winter, with the occurrence of precipitation systems known as Easterly Wave Disturbances (EWD) (Pontes da Silva, 2011; Gomes et al., 2015). Therefore, we expected the dry season to occur during the austral summer, as observed according to the method used in this study.

The three metropolises located in the extreme north of Brazil have dry season during September-October-November, since the region is not under the influence of the main meteorological systems that generate rainfall in the Intertropical Convergence Zone (ITCZ). For Teresina and Manaus, the dry period was observed between July and September. Among the metropolises located in the South region, only Porto Alegre does not have the dry season in the austral winter. Its dry season runs from November to January, a situation possibly related to the rapid passage of frontal systems in the region.

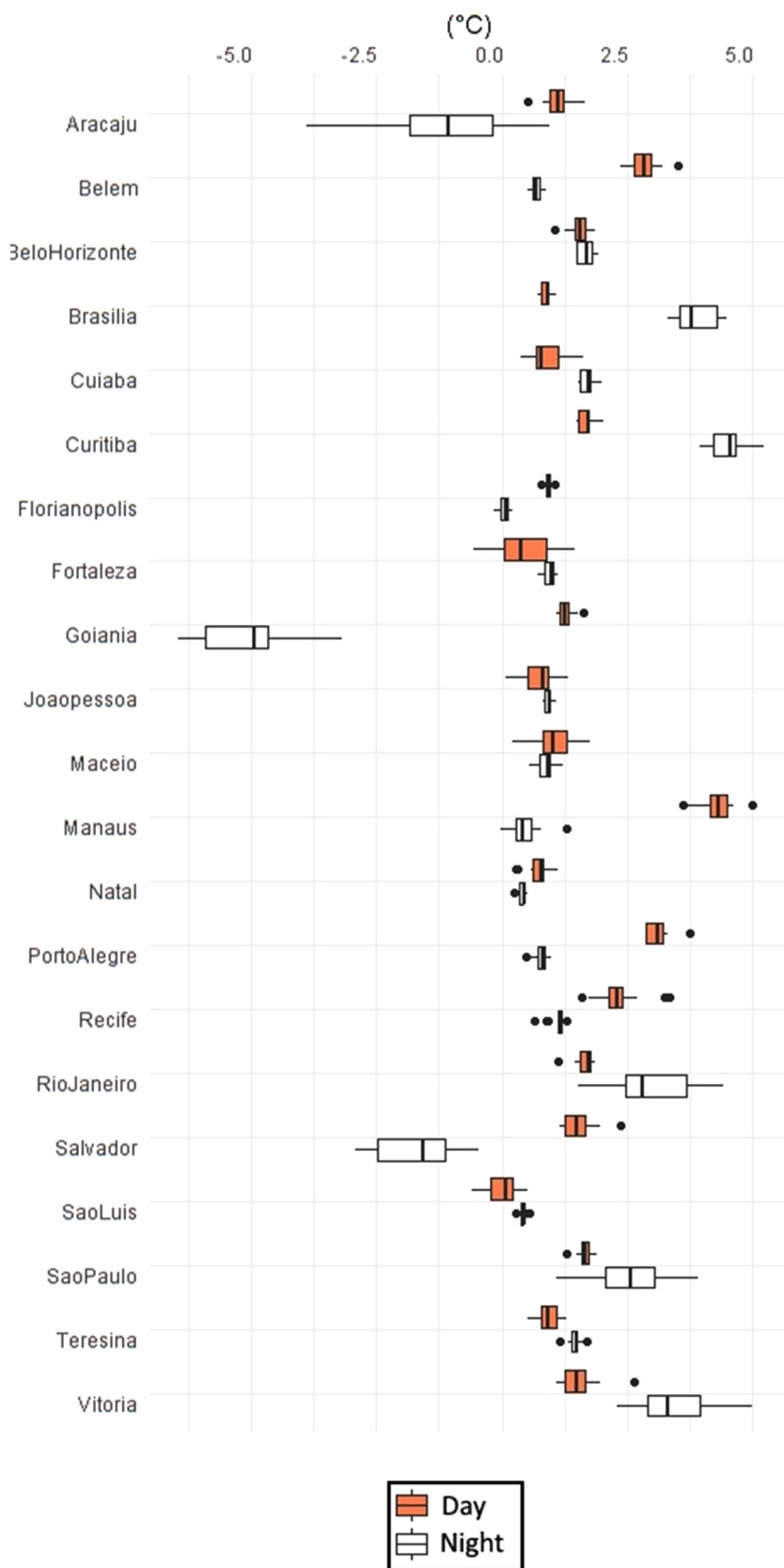
Fig. 4 shows the average values of the surface temperature during the day and night. A total of 16 metropolitan regions presented daytime temperatures above 30 °C, and the highest values were above 35 °C in the metropolitan region of Teresina, followed by Fortaleza, both located in the Northeast. These cities are located at low latitudes and the dry season occurs during the winter-spring

Table 3

Average values of Δ_{NDVI} , Δ_{Albedo} , and daily and nightly average UHI and trend of UHI, during the dry season, between 2000 and 2016, for each Brazilian metropolis analyzed.

Metropolitan Area	Δ_{NDVI}	Δ_{Albedo}	Diurnal		Nocturnal	
			UHI mean (°C)	UHI Trend (°C/decade)	UHI mean (°C)	UHI Trend (°C/decade)
Aracaju	-0.094	0.027	1.055	**0.090	-1.052	1.150
Belém	-0.157	0.022	2.814	0.160	0.678	0.060
Belo Horizonte	-0.182	0.006	1.525	**0.140	1.665	-0.120
Brasília	-0.180	0.010	0.871	**0.090	3.869	0.037
Cuiabá	-0.071	0.007	0.867	**0.270	1.691	0.054
Curitiba	-0.183	0.011	1.689	**0.160	4.465	0.088
Florianópolis	0.015	0.040	0.921	-0.010	0.038	-0.011
Fortaleza	-0.113	0.027	0.435	**-0.730	0.930	-0.170*
Goiânia	-0.095	-0.006	1.276	0.000	-5.131	-0.660
João Pessoa	-0.081	0.040	0.721	0.010	0.906	0.020
Maceió	-0.020	0.035	1.043	0.040	0.867	-0.110
Manaus	-0.060	0.040	4.261	**0.330	0.438	-0.080
Natal	-0.264	0.022	0.730	**-0.200	0.390	0.012
Porto Alegre	-0.175	0.008	3.089	**0.280	0.785	0.086
Recife	-0.097	0.033	2.322	0.080	1.094	-0.050
Rio de Janeiro	-0.194	0.022	1.637	**0.200	2.875	0.210
Salvador	-0.075	0.033	1.518	**0.230	-1.734	0.600
São Luís	-0.076	0.015	0.005	-0.050	0.410	-0.030
São Paulo	-0.216	0.009	1.639	**0.130	2.615	0.600
Teresina	-0.095	0.009	0.904	**-0.200	1.441	0.008
Vitoria	-0.114	0.020	1.496	0.070	3.477	-0.500

* Trend with a significance level of 95%.



(caption on next page)

Fig. 5. Boxplot of the daytime and nighttime heat island intensities of the Brazilian metropolises studied.

period. Therefore, especially during the spring, overheating may have a negative impact on the population. The lowest nocturnal values occurred in the metropolitan regions of Goiânia, Florianópolis, and Curitiba, all with the dry season occurring during the austral winter, with average temperatures below 15 °C.

3.2. Day and night variation of UHI

During the daytime, urban surfaces absorb more radiation than the urban edge areas. This radiation is converted into thermal energy and re-emitted in longer waves in smaller quantities during the night. This is due to the multiple reflections of the radiation confined between the buildings in urbanized areas, while in open spaces there is a rapid radiative cooling because no confinement of heated air occurs (Rizwan et al., 2008). After calculating the differences between T_{urban} and T_{edge} for the studied metropolises, we applied the t-test to classify the UHI effect only for the metropolitan areas in which the temperature differences were statistically significant.

The t-test results showed that all metropolises presented a significant difference between the edge and urban area temperatures during the studied years, both for the nocturnal and diurnal periods, indicating the presence of the UHI effect. It is important to mention that the MOD11A2 product provides information only for land areas excluding the pixels present in large lakes or over the ocean. This feature ensures that the average values obtained within the edge region or urban core are not influenced by the presence of water bodies.

Regarding the UHI trends of the Brazilian metropolitan areas, in the daytime, 13 metropolises showed significant positive trends. Among them, Manaus and Porto Alegre had the highest values of heating trends (0.3 °C/decade). On the other hand, the metropolitan areas of São Paulo and Rio de Janeiro, the largest metropolises in Brazil, showed significant positive trends of 0.13 °C/decade and 0.2 °C/decade, respectively. The metropolises of Aracaju and Brasília underwent less intense heating, with a trend of 0.09 °C/decade.

For the night period, only Fortaleza showed a significant negative trend, indicating a reduction of 0.17 °C/decade, possibly due to gradual occupation of the edge area or greater afforestation in the urban area, both situations leading to a reduction in the UHI values with time (Table 3).

For the daytime UHI (Fig. 5), Manaus registered the highest value among all metropolises, with an average intensity of +5 °C, followed by Belém and Porto Alegre, both with values close to +3 °C. According to Souza and Alvalá (2014) and Corrêa et al. (2016), one of the main causes of the large contrast observed in metropolitan areas located in the North region of Brazil is that the border areas are occupied by the Amazon Forest, which presents drastically different energy balance characteristics than urban environments.

Large metropolitan areas such São Paulo and Rio de Janeiro showed lower UHI intensities, close to +1.5 °C, and also higher Δ_{NDVI} values (−0.22 for São Paulo and −0.19 for Rio de Janeiro) (Table 3), indicating there is a large difference of areas covered by vegetation between the urban and border regions. According to Spinoza (2017), the urban environment has a direct influence on local circulation, which in turn is directly influenced by Δ_{NDVI} values.

However, the high Δ_{NDVI} values were not accompanied by elevated diurnal UHI values. On the other hand, the nocturnal UHI presented higher values for São Paulo and Rio de Janeiro, which will be discussed in the following paragraphs. Regarding Δ_{Albedo} (Table 3), a value of 0.009 was found for the metropolitan area of São Paulo, which may be related to the occupation of urban edge regions as well as the low plant cover.

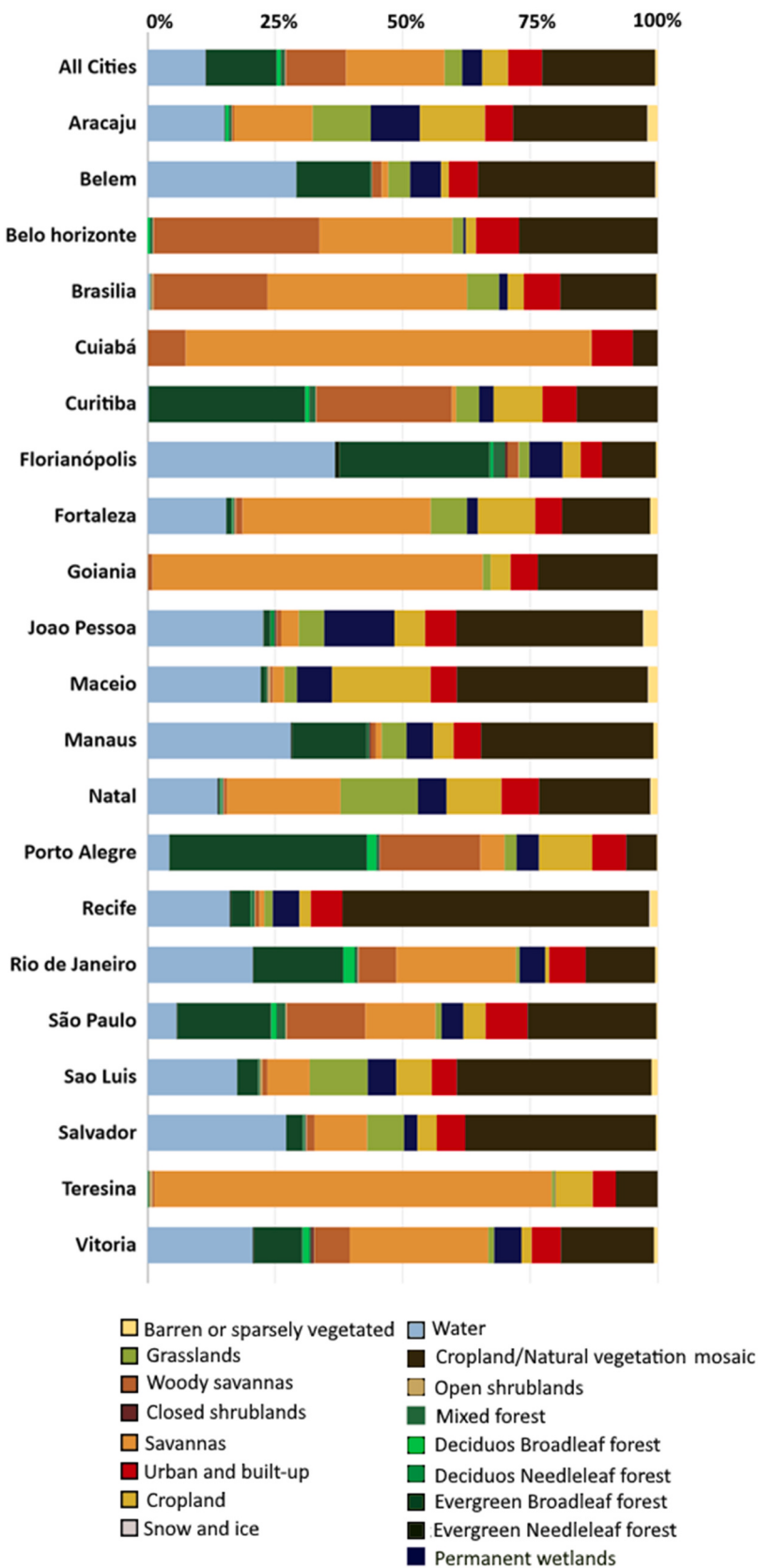
Several authors have mentioned that nocturnal UHI generally presents higher intensities (Oke, 1988; Tan et al., 2008; Sobstyl et al., 2018), since the thermal mass of buildings, heated during the day, slowly releases the heat absorbed in the form of long-wave radiation. The results obtained in this study indicate the influence of the built density on the higher intensities of nocturnal UHI for large metropolises. Among them are Curitiba and Brasília, which recorded the highest UHI intensities, above 3 °C, followed by São Paulo, Rio de Janeiro, and Vitória, with values between 2.5 and 3 °C.

This result might be related to the different cooling rates of the urban and non-urban areas during the night. These are influenced by the high density, intense verticalization and thermal properties of the building materials, which absorb thermal energy close to the surface and raise nocturnal temperatures, more intensely in the dry season (Kim and Baik, 2002; Zhang et al., 2012; Santana, 2014; Werneck, 2018). The five metropolises with the highest nocturnal UHI had lower albedo values in the urban cores, as well as lower average Δ_{Albedo} , meaning less reflection of the incident energy throughout the day, which is accumulated during the day and gradually released as long-wave radiation at night, increasing the UHI values.

The metropolises of Salvador, Aracaju, and Goiânia registered negative values for nocturnal UHI. One possible cause of this result is the lower presence of border vegetation compared to the urban core, which can cause a reduction of evapotranspiration outside the urban core, mainly in the dry season. On the other hand, the urban areas with greater presence of vegetation and available water have higher evapotranspiration rates, consequently altering the sensible and latent heat fluxes, keeping the surface temperature cooler than in the border area (Cardoso, 2017).

For a better understanding of the UHI intensities, we verified the proportion of the different classes of LULC on the edges of the studied metropolitan areas (Fig. 6). Considering all the metropolises in Brazil, there was predominance of vegetation cover: 30% of these areas are occupied by savannas, 22% by natural vegetation and cropland and 14% by dense forests, with percentage changes between metropolises.

Analysis of the UHI by regions indicated that the Southeast metropolises presented diurnal UHI above 1.5 °C. The metropolitan area of Vitória recorded nocturnal UHI above 3 °C, followed by São Paulo and Rio de Janeiro. According to Paula (2015), Vitória has changed in both the diurnal and nocturnal thermal patterns due to modifications in urban land-use. Rio de Janeiro has also changed the



(caption on next page)

Fig. 6. Stacked column chart of proportion by land-use class of Brazilian metropolitan areas.

thermal pattern because of increased constructed density (Sena et al., 2014; de Meireles et al., 2014).

São Paulo registered positive UHI during the day and night, in the latter case with greater intensity. This is consistent with the results found by Ribeiro et al. (2016) and Umezaki and Ribeiro (2019). This implies that the residents are at risk of overheating, according to Duursma (2002). The causes are modifications in the energy balance, attributed to the potential of urban buildings to store energy received during the day and release it during the night, in addition to other anthropogenic sources.

São Paulo has high demographic growth and urban expansion rates, encroaching on the last remnants of natural vegetation, contributing to thermal impacts (Takiya, 2002). In addition, other studies have found that the São Paulo metropolitan region is going through a process of rising temperatures. Nobre et al. (2011) and Umezaki and Ribeiro (2019) evaluated the air temperature in the São Paulo metropolitan region in the twentieth century and verified an increase of 2 °C to 3 °C in relation to the average temperature in the previous century. These observations are in agreement with our results, which indicate a positive trend in the UHI (0.13 °C/decade), resulting in continued urban heating if current land-use patterns are maintained.

The metropolitan areas in the North region, Belém and Manaus, presented high daytime heat island values, corroborating the results of Souza and Alvalá (2014), who analyzed the regions using climate modeling and also observed temperature anomalies. For the daytime period, the marked values can be related to the high density of buildings, which retain the sensible heat related to low humidity in the dry period, aggravating discomfort in these metropolises (Wienert and Kuttler, 2005; Krehbiel et al., 2016).

The Manaus metropolitan area, which recorded the highest heat island intensity of the metropolises, has about 33.8% of its edge occupied by natural vegetation and cropland, and about 14% with dense forest cover, explaining the high urban thermal contrast. For the night period, the reduction in UHI intensity might be associated with the presence of the Amazon Forest, which raises the proportion of latent heat in the energy balance and reduces the temperature contrasts between the border and urban core (Foley et al., 2003).

Among the metropolises from the South region, Porto Alegre recorded one of the highest values of daytime UHI, which during the night declined to less than 1 °C, implying low retention of the radiation received during the day. This pattern was similar in Curitiba, which presented a daytime UHI above +1.5 °C. However, Curitiba showed an increase of the UHI from day to night of about 3 °C, reaching 4.4 °C, the highest nocturnal UHI intensity among all metropolises. The reason for this might be linked to dense urban geometry and a border area occupied by woody savannas (26.54%) and dense forests (30.64%), which change albedo and lead to disparities in the surface energy balance.

Of the cities in the Midwest region, Brasilia stood out with nocturnal UHI above +3 °C, while Goiania had a negative UHI of -5 °C. In this region, the metropolises are becoming more densely developed, which leads to large areas of exposed soil and high density of concrete and asphalt, retaining more heat and raising their temperatures (Werneck, 2018; Santana, 2014).

In the city of Goiania, 64.87% of the border area is occupied by savanna and 23.52% by cropland, with sparse natural vegetation. As the difference between urban and border albedo was small ($\Delta_{\text{Albedo}} = -0.006$), the vegetation must play a fundamental role in heat

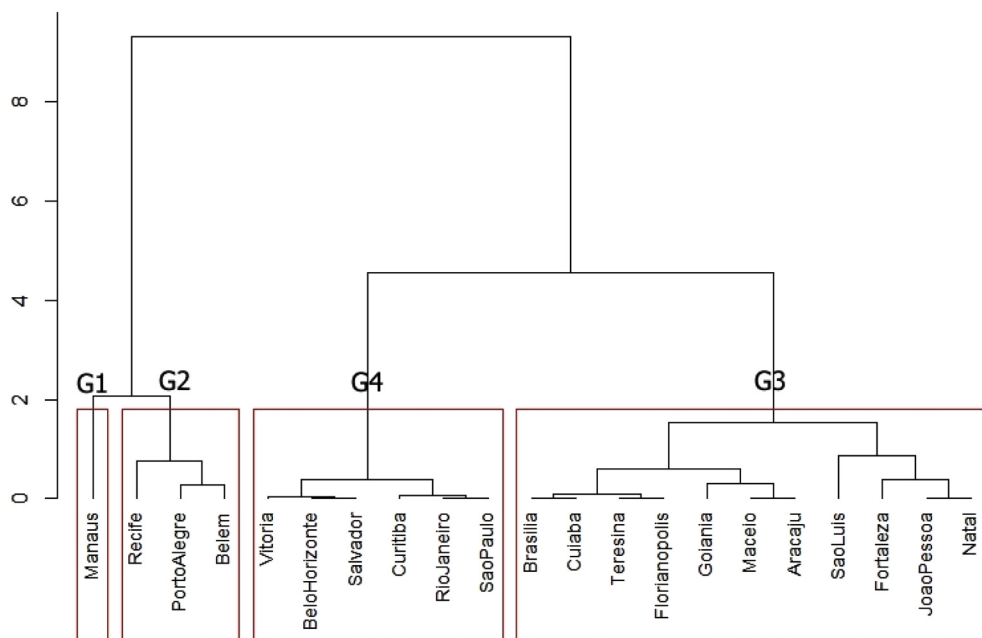


Fig. 7. Clusters according to the daytime UHI intensity. Metropolitan groups delimited in red rectangles. (For interpretation of the references to colour in this figure legend, the reader is referred to the web version of this article.)

retention and sensible heat fluxes, impacting the temperature contrast, especially in the dry season. This aspect, together with intra-urban characteristics, may influence the energy balance and the differentiation of temperatures in the nocturnal period (Kruger and Gonzalez, 2016).

For the Amazon basin, Marengo (2003) reported warming on the order of $+0.85^{\circ}\text{C}/100$ years, which is an alarming scenario compared to the estimate of Victoria et al. (1998), which was $+0.56^{\circ}\text{C}/100$ years. For the city of Manaus, a warming trend of $+0.3^{\circ}\text{C}/\text{decade}$ was observed (Table 3), which is greater than the results obtained by Marengo (2003) and Victoria et al. (1998). Our estimates show that the temperature in Manaus is increasing at the greatest rate in the Amazon Basin.

3.3. Cluster analysis

After analyzing the trends of the UHI intensities in Brazilian metropolises, we conducted a cluster analysis to group those presenting historic similarity of UHI. This step was important to verify whether common characteristics among metropolises influence the values found. An overview of the clusters formed indicates a significant inverse impact of vegetation and surface albedo in relation to UHI.

For the daytime period, four clusters were identified (Fig. 7). The cluster G1 was formed only by the city of Manaus, which presented the highest UHI value of all metropolises, $+4.45^{\circ}\text{C}$. Considering the environmental variables, Manaus presented one of the greatest differences in albedo levels, with Δ_{Albedo} of $+0.040$ (Table 3), meaning that the urban area reflects 4% more shortwave radiation than the dense Amazonian forest.

The cluster G2 contains Recife, Belém and Porto Alegre, which have in common the fact that their dry season occurs during the spring and summer, causing higher air temperature and increased UHI effect. In the dry season, the vegetation in the border areas becomes less dense, which leads to smaller Δ_{Albedo} values, of 0.02 (Table 3). Moreover, these metropolises have the highest contrasts of afforestation among the capitals (Δ_{NDVI} near -0.15).

The metropolises in cluster G3 have daytime UHI below 1°C , the lowest values among those studied. This group contains the capitals of the Northeast region besides Brasília and Florianópolis. They all are characterized by high temperatures during the dry months. This finding corroborates the observations of Arnfield (2003) and Ward et al. (2016), that drier and warmer metropolises generally have lower UHI magnitudes. Nevertheless, this result does not mean a change has occurred in the impacts caused by urban development, aggravated by the lower presence of vegetation (Monteiro and Silveira, 2013).

Cluster G4 contains the largest Brazilian metropolitan areas: São Paulo, Rio de Janeiro, Belo Horizonte, Curitiba, and Salvador, along with Vitória, Curitiba, Goiânia and Aracaju. In this cluster, mean UHI values greater than 1.5°C per decade were identified, and the lowest negative Δ_{NDVI} values as well. A common factor among these metropolitan regions is the higher built density, which increases the surface roughness and reduces the heat dissipation through ventilation (Lombardo, 2009). According to Kruger (2016), urban geometry is the aspect that most contributes to the development of the UHI effect.

Another aspect is the lower presence of urban vegetation cover compared to the respective border areas. This important aspect directly affects the energy balance, since impermeable surfaces have greater heat gain during the day, increasing the temperature differences (Oke, 1987; Gallo et al., 1993; Weng et al., 2004). The lack of vegetation alters the partition of energy flows on the surface,

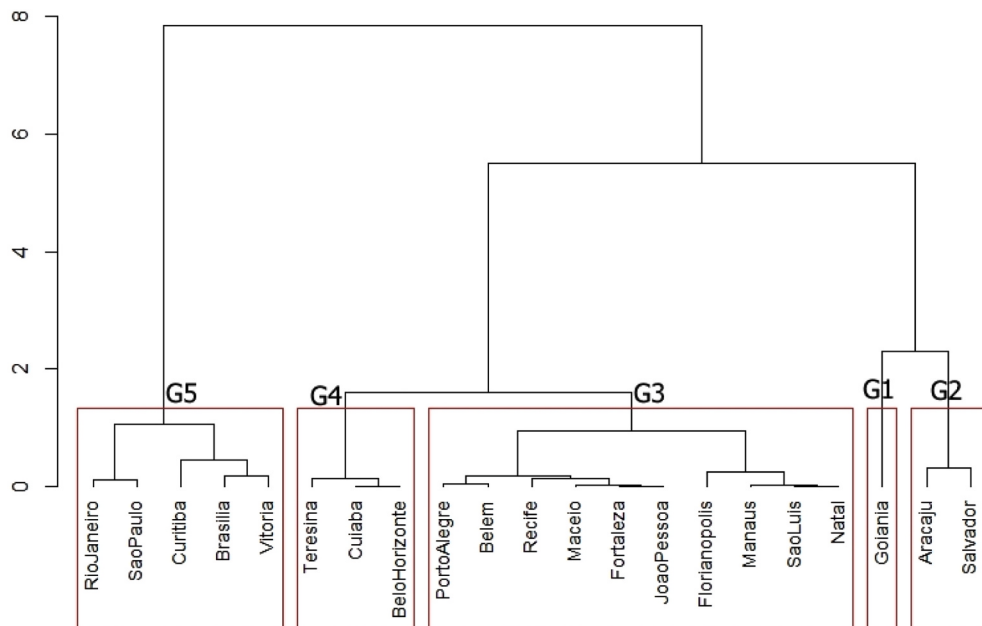
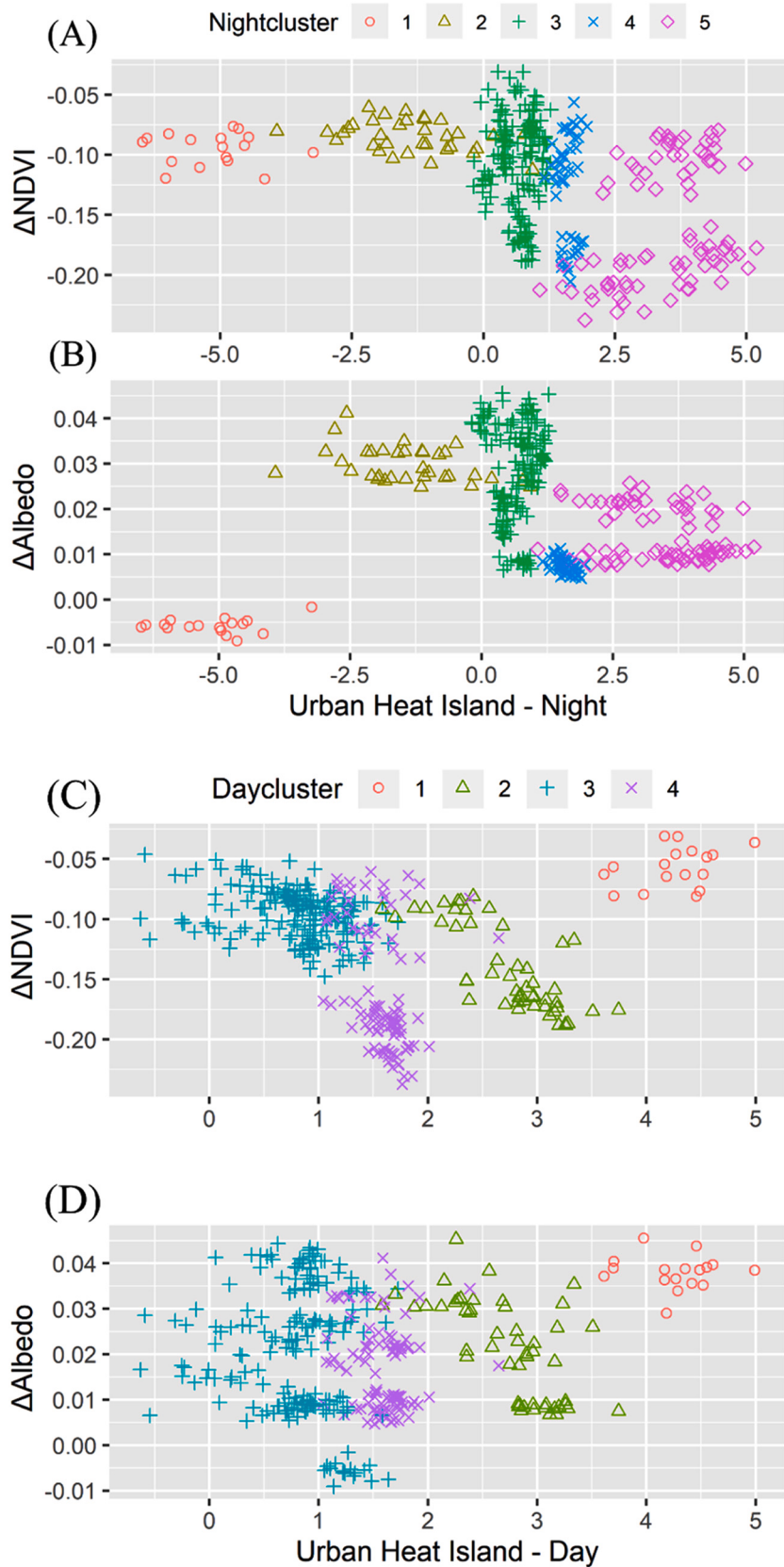


Fig. 8. Clusters according to the nighttime UHI intensity. Metropolitan groups delimited in red rectangles. (For interpretation of the references to colour in this figure legend, the reader is referred to the web version of this article.)



(caption on next page)

Fig. 9. Scatter plots of UHI cluster groups with Δ_{Albedo} and Δ_{NDVI} . Plots A and B denote the nighttime UHI values and plots C and D the daytime UHI values.

reducing soil evaporation and latent heat flow, consequently increasing the sensible heat flow (Peng et al., 2012; Imhoff et al., 2010). In addition, the greater urban density brings an increase in the levels of pollutants in the air (Lai and Cheng, 2009). The presence of these aerosols can lead to an increase of absorption of long-wave radiation (Oke, 1982), which potentially warms the atmosphere.

For the nocturnal period, five clusters were obtained (Fig. 8). Cluster G1 contains only Goiânia, which presented a negative UHI, -5.13°C . This result could be a combination of two factors. The first is related to the negative difference of albedo between the urban core and its border (Δ_{Albedo} of -0.006), meaning greater reflection of energy in the edge region. The second is the small amount of vegetation both in the urban core and edge area.

The combination of these factors causes small absorption of radiation during the day and rapid loss of long-wave radiation during the night. This condition modifies the energy balance, causing greater loss of energy in urban areas compared to the edge, resulting in lower night temperatures in the core (Kruger and Gonzalez, 2016).

The negative heat island formation observed in both groups may be linked to urban geometry, which according to Sobstyl et al. (2018) is one of the factors influencing thermal capacity and consequently the heat loss velocity, thus altering the intensity of nocturnal UHI.

Cluster G3 includes all metropolises with nocturnal UHI below $+1^{\circ}\text{C}$ (Fig. 8). Manaus, Belém and Porto Alegre are highlighted for presenting high variation between UHI in diurnal and nocturnal periods (Fig. 5). This result can be considered a positive aspect for the residents of these metropolises, since it indicates cooling at night and consequent better surface energy balance. Cluster G4 contains metropolises with an average nighttime UHI of $+1.5^{\circ}\text{C}$, but with low Δ_{Albedo} levels, and a dry period with very low Δ_{NDVI} levels (Table 1).

Cluster G5 contains the metropolises with the highest positive nighttime UHI values and low levels of Δ_{Albedo} (Table 3). This cluster is composed of the largest Brazilian metropolitan areas (São Paulo, Rio de Janeiro, Brasília, Curitiba, and Vitória). The thermal contrast in Curitiba reaches $+4.46^{\circ}\text{C}$, followed by Brasília and Vitória, with $+3.8^{\circ}\text{C}$ and $+3.4^{\circ}\text{C}$, respectively. The high values can be related to the high urban density, which absorbs radiation during the day and emits long-wave radiation during the night.

To understand the behavior of the UHI effect in relation to Δ_{NDVI} and Δ_{Albedo} , we constructed scatter plots (Fig. 9). The figures showed that the relationship between the intensities of UHI, both nocturnal and diurnal, is not direct, confirmed by the fact that different variations of Δ_{NDVI} and Δ_{Albedo} were observed for the same values of UHI. A detailed assessment indicates there are intrinsic characteristics of each metropolis that directly influence the UHI phenomenon. Among them is the high constructive density using materials with low albedo and high thermal inertia. This condition traps more thermal energy, associated with the contrast in the presence of vegetation between the urban environment and its surroundings, meaning higher temperatures in the urban area than in border areas.

For the daytime period (Fig. 9 C and D), the UHI intensities are directly related to aspects of land-use and energy balance of the urban surface. Cluster G1, composed only by Manaus, presented the highest UHI values, as previously mentioned. Also, the Δ_{Albedo} value (Fig. 9 D) is more representative of the intensity of the UHI, since the Δ_{NDVI} (Fig. 9 C) values are not high.

The metropolises contained in cluster G2 presented greater Δ_{NDVI} than Manaus. Their edges are predominantly occupied by croplands and natural forests, leading to positive Δ_{Albedo} values. In comparison to cluster G1, the lower values of UHI can be attributed to the greater presence of vegetation in the urban area, supporting its importance as a mitigating element of the phenomenon.

Cluster G3 registered lower values of UHI compared to the other groups. However, this group presented the highest Δ_{Albedo} , which means that the urban cores of some metropolises have greater energy reflection than the borders, which are mainly covered by cropland/natural vegetation mosaic. Cluster G4 is composed of the most populated Brazilian metropolises. However, these did not present high UHI values, since the edge regions are also less vegetated and are marked by encroachment of urban sprawl, reducing the temperature differences.

For the night period (Fig. 8 A and B), the values of UHI are influenced by the balance of daytime energy, directly associated with greater or lesser heat retention during the day, depending on the characteristics of each metropolis. Clusters G1 and G2 present negative UHI values. The edges of these metropolises are mainly occupied by savanna and cropland areas with sparse natural vegetation. This situation leads to both negative Δ_{Albedo} and Δ_{NDVI} values, which was not observed for the other groups. Special attention should be given to Goiânia, which presented the lowest Δ_{Albedo} value and Δ_{NDVI} value similar to the other capitals, meaning faster heat loss in the urban core than the edge.

Cluster G3 contains 50% of the studied metropolises, with UHI values between 0 and 1°C . These presented wide variation in the values of Δ_{NDVI} and Δ_{Albedo} , while the cities in cluster 4 have UHI values above 1°C , and predominance of savannas and croplands in the surrounding areas. Cluster G5 consists of the largest Brazilian metropolises. Among them are São Paulo and Rio de Janeiro, which registered the highest values of nocturnal UHI. This is associated with the high built density of these metropolises, which retains heat even during the night.

4. Discussion

The results of the daytime trend reveal a worrying reality for large Brazilian metropolises, because if the current urban occupation trend is maintained, in 50 years there will be an average increase of UHI of 1°C , directly affecting all residents and infrastructure systems. The presence of the UHI effect has varied impacts on the residents, such as aggravating the spread of various diseases.

According to Ribeiro et al. (2016), high temperature directly impacts health, posing a risk especially to more vulnerable groups like old people and children, and also inhabitants of precarious zones. The diseases whose incidence increases due to higher heat are those borne by vectors, which benefit from warmer climate. Among these diseases are dengue, zika and leptospirosis and those caused by other arboviruses (Coelho-Zanotti and Massad, 2012; Hansen et al., 2015; Rochlin et al., 2013).

Among the studied metropolises, those located in the North and Northeast regions already have a high number of registered arbovirus cases (Mastrangelo, 2016; Johansen, 2014; Pimenta, 2015; Segata, 2016), a situation that can worsen if the UHI levels are not mitigated.

Heatwaves together with the UHI effect raise energy demands for air conditioning, especially for people more sensitive to heat (elderly and children) (Dhalluin and Bozonnet, 2015). As a result, this can lead to a trend of increasing energy consumption, as discussed by Souza et al. (2009) and Calice et al. (2017).

More than half of the studied metropolises are located along the coastline. The cluster analysis revealed no daytime grouping of these cities, probably because of the particular aspects of each one, meaning great variation in the UHI intensity. In the nocturnal period, the cluster G3 contains most of the coastal metropolises studied. All these present UHI values below 1 °C, likely reflecting the cooling influence of nighttime onshore sea breezes.

Considering the urban geometry, Sobstyl et al. (2018) described a relation between the UHI intensity and the layout of the urban road network. The authors commented that areas with straight and perpendicular streets, which are consequently denser, have the potential to absorb a large amount of heat. Within the studied metropolitan regions, Brasília and São Paulo are examples of this characteristic, with UHI values. On the other hand, São Luís and Salvador, which have irregular layouts, lose heat more easily, reducing the UHI impact.

In addition to the urban geometry layout, different cooling rates of urban and non-urban areas are affected by the thermal properties of the surface. An explanation for the distinct nocturnal UHI effects found in different metropolises is the thermal capacity of the urban environment, which has variations due to geometry and the predominant construction materials. Thus, further studies are needed, such as with smaller scales, to understand the intrinsic characteristics of each metropolis.

This happens especially due to the high thermal inertia of some materials, which leads to a greater retention of heat and slow release at night. Brasília fits this description, where the UHI effect is still present during the night, possibly due to the large areas covered by concrete and asphalt. This can explain the negative nocturnal UHI values found in some metropolises.

To mitigate the UHI effects, numerous strategies can be adopted, such as changes of urban morphology, especially in the urban expansion areas (Tam et al., 2015; Wong et al., 2011); development of green infrastructure or expansion of areas covered by vegetation (Tzoulas et al., 2007); and expansion of areas with highly reflective pavements (Akbari and Matthews, 2012; Santamouris, 2013). The basic principle of these strategies generally depends on the modification of the surface energy balance in the constructed spaces, where, the adoption of high albedo paving reflects more direct solar radiation, while the planting of urban vegetation tends to redistribute thermal energy and affect the latent heat (Wang, Bou-Zeid and Smith, 2013).

5. Conclusions

This study evaluated the behavior of the day and night UHI effect using different remote sensing products from the MODIS sensor. The analyses were performed during the dry season in the main Brazilian metropolitan areas, between 2000 and 2016, to identify the presence and trend of the phenomenon, as well as to identify the similarities and differences among metropolises. To understand the characteristics of the UHI effects analyzed, biophysical aspects (surface albedo and NDVI) of each metropolitan area were evaluated to compare their urban area with the respective edges.

The results demonstrated the presence of the UHI effect in all the metropolitan areas, with intensities varying according to the period of the day. In Manaus, the highest daytime intensity of the phenomenon was observed, with +4.26 °C, and an increase trend of +0.3 °C/decade. These results can be explained by the city's compact urban form and the surrounding presence of tropical rainforest, raising the temperature contrasts. It is also important to note that the Manaus metropolitan region has the highest dwelling density among the metropolises studied, which possibly contributes to the retention of thermal energy.

For the nighttime, the metropolitan area of Curitiba, one of the largest in the South region of Brazil, presented the highest UHI value (+ 4.4 °C), but without a significant trend. The largest two Brazilian metropolises, São Paulo and Rio de Janeiro, showed daily UHI values above 1.5 °C, and nighttime UHI above 2.5 °C. These results indicate that these metropolises are continuously overheated regardless of the period of the day, aggravating the health risks of the population, which exceeds 10 million inhabitants in each city. It is possible to associate the results found with the built density and the use of building materials with greater thermal inertia, such as concrete and asphalt, conditions that contribute to heat retention.

We identified that about 60% of the studied areas presented positive trends in the values of the daytime UHI. The specificities of each metropolitan area regarding the biophysical aspects of Δ_{NDVI} and Δ_{Albedo} allowed understanding the influence of the vegetation cover within and surrounding the urban regions on the UHI values. The results obtained based on the groupings show that the physical dimension of a metropolis is not the main determinant of the intensity of the phenomenon. Biophysical characteristics must be taken into account, since they affect the UHI intensity as much as the size of the metropolitan area. Other factors, such as urban population density and urban built density, which indicate the form of land occupation, should also be highlighted.

Some limitations should be considered regarding the use of data from the MODIS sensor, since the low spatial resolution does not allow intra-urban detailing of the phenomenon, instead only allowing dichotomous analysis of temperatures between urban and non-urban regions. Hence, it was not possible to observe individualized intra-urban characteristics of each metropolis, so further investigation is warranted. However, it should be noted that the database used provides wide spatial coverage and good temporal

resolution. In addition, the easy access to images and recent developments in image processing techniques make remote sensing attractive for estimating and continuously monitoring temperature values in urban environments.

A more in-depth investigation is necessary of aspects of urban occupation, on the intra-urban scale, in the metropolises that recorded the highest heat island values, both diurnal (Manaus, Belém, Porto Alegre, Recife) and nocturnal (São Paulo, Brasília, Curitiba, Rio de Janeiro, Vitória). The Goiânia metropolitan area also needs more detailed research to identify the causes of the negative nocturnal UHI value. To achieve this result, numerical modeling with high temporal and spatial resolution should be used. The relationship between the heat island effect and land-use characteristics indicates that mitigating the phenomenon requires:

- implantation or expansion of green areas in the urban core, in order to modify the energy balance, in addition to ensuring higher levels of relative humidity and soil moisture, thereby reducing surface and air temperatures; and.
- elevation of the average albedo of urban surfaces, by altering the type of pavement and roof materials.

It is necessary to consider the realities of each city so that solutions can be adopted at appropriate scales. Their effectiveness depends entirely on local environmental conditions, including climatology, geography and surface topology, always seeking to reduce temperatures in the urban environment and ensure the welfare of the population.

Declaration of Competing Interest

None.

Acknowledgments

The authors gratefully acknowledge the financial support to the first author granted by the CAPES 001 funding code and thank the reviewers for their contribution.

References

- Akbari, H., Matthews, H.D., 2012. Global cooling updates: reflective roofs and pavements. *Energy Buildings* 55, 2–6.
- Anderson, B.G., Bell, M.L., 2009. Weather-related mortality: how heat, cold, and heat waves affect mortality in the United States. *Epidemiology* (Cambridge, Mass.) 20 (2), 205.
- Arnfield, A.J., 2003. Two decades of urban climate research: a review of turbulence, exchanges of energy and water, and the urban heat island. *Int. J. Climatol.* 23 (1), 1–26.
- Bourscheidt, V., Pinto Jr., O., Naccarato, K.P., 2016. The effects of São Paulo urban heat island on lightning activity: decadal analysis (1999–2009). *J. Geophys. Res.* 121 (9), 4429–4442.
- Buyantuyev, A., Wu, J., 2010. Urban heat islands and landscape heterogeneity: linking spatiotemporal variations in surface temperatures to land-cover and socioeconomic patterns. *Landscape Ecol.* 25 (1), 17–33.
- Cadenasso, M.L., Pickett, S.T., Schwarz, K., 2007. Spatial heterogeneity in urban ecosystems: reconceptualizing land cover and a framework for classification. *Front. Ecol. Environ.* 5 (2), 80–88.
- Calice, C., Clemente, C., Salvati, A., Palme, M., Inostroza, L., 2017. Urban Heat Island effect on the energy consumption of institutional buildings in Rome. In: IOP Conference Series: Materials Science and Engineering (Vol. 245, No. 8, p. 082015). IOP Publishing.
- Campelo, J.C., Leal Junior, J.B.V., Sombra, S.S., Magalhães, A.J.S., Gomes, F.C., Alves, A.O., Gondim, F.L., Castro, E.S., Alves, J.M.B., 2018. Study of the phenomena of urban heat island in northeast of Brazil in the states of Ceará and Rio Grande do Norte. *Int. J. Develop. Res.* 8 (2), 18954–18961.
- Cardoso, L.M.G., 2017. Estudo do Microclima urbano a partir de plataformas de coleta de dados(PCD's) da fachada sudeste de salvador. In: Dissertação (Mestrado em Engenharia Ambiental). UFBA, Escola Politécnica – in Portuguese.
- Carlson, T.N., Ripley, D.A., 1997. On the relation between NDVI, fractional vegetation cover, and leaf area index. *Remote Sens. Environ.* 62 (3), 241–252.
- Cavalcanti, I.F.A., Kousky, V.E., 2003. Climatology of South American cold fronts. In: International Conference on Southern Hemisphere Meteorology and Oceanography (Vol. 7, p. 2003). Wellington, New Zealand. Proceedings... Wellington: Amer. Meteor. Soc., 2003.
- Clinton, N., Gong, P., 2013. MODIS detected surface urban heat islands and sinks: global locations and controls. *Remote Sens. Environ.* 134, 294–304.
- Coelho-Zanotti, M.S.S., MASSAD, E., 2012. The impact of climate on leptospirosis in São Paulo, Brazil. *Int. J. Biometeorol.* 56, 233–241.
- Coltri, P.P., Junior, C.M., Velasco, G.D.N., Ferreira, N.J., Freitas, S., 2009. Influência do uso e Cobertura do Solo nas ilhas de calor Local e regional no município de Piracicaba, São Paulo. Simpósio Brasileiro de Sensoriamento Remoto 14, 639–646.
- Constantinescu, D., Cheval, S., Caracaş, G., Dumitrescu, A., 2016. Effective monitoring and warning of Urban Heat Island effect on the indoor thermal risk in Bucharest (Romania). *Energy Buildings* 127, 452–468.
- Correa, L. V., Análise dos efeitos térmicos da superfície na cidade de Belém-Pará-Brasil utilizando imagens de satélite. 2011. 80f (Doctoral dissertation, Dissertação (Mestrado em Ciências Ambientais)–Universidade Federal do Pará, Belém).
- de Meireles, V.H.P., de Almeida França, J.R., Peres, L.F., 2014. Um estudo do fenômeno da Ilha de Calor urbana na Região Metropolitana do Rio de Janeiro (RMRJ). *Anu. Inst. Geocienc.* 37 (2), 180–194.
- Deilami, K., Kamruzzaman, M., Liu, Y., 2018. Urban heat island effect: a systematic review of spatio-temporal factors, data, methods, and mitigation measures. *Int. J. Appl. Earth Obs. Geoinf.* 67, 30–42.
- Dhalluin, A., Bozonnet, E., 2015. Urban heat islands and sensitive building design—a study in some French cities' context. *Sustain. Cities Soc.* 19, 292–299.
- Dousset, B., Gourmelon, F., 2003. Satellite multi-sensor data analysis of urban surface temperatures and landcover. *ISPRS J. Photogramm. Remote Sens.* 58 (1–2), 43–54.
- Du, H., Wang, D., Wang, Y., Zhao, X., Qin, F., Jiang, H., Cai, Y., 2016. Influences of land cover types, meteorological conditions, anthropogenic heat and urban area on surface urban heat island in the Yangtze River Delta urban agglomeration. *Sci. Total Environ.* 571, 461–470.
- Duursma, E., 2002. Rainfall, River Flow and Temperature Profile Trends: Consequences for Water Resource. Heineken, Amsterdam, Netherlands.
- Dwivedi, A., Khire, M.V., 2018. Application of split- window algorithm to study Urban Heat Island effect in Mumbai through land surface temperature approach. *Sustain. Cities Soc.* 41, 865–877.
- Foley, J., Costa, M., Delire, C., Ramankutty, N., Snyder, P., 2003. Green Surprise? How Terrestrial Ecosystems Could Affect Earth's Climate. *Front. Ecol. Environ.* 1, 38–44.
- Friedl, M.A., McIver, D.K., Hodges, J.C., Zhang, X.Y., Muchoney, D., Strahler, A.H., Baccini, A., 2002. Global land cover mapping from MODIS: algorithms and early results. *Remote Sens. Environ.* 83 (1–2), 287–302.

- Fuckner, M.A., Moraes, E.C., Florenzano, T.G., 2009. Processamento de dados multiespectrais termais aplicado à análise espaço-temporal dos padrões de temperatura da superfície nas Regiões Metropolitanas de São Paulo e Rio de Janeiro. In: XIV Simpósio Brasileiro de Sensoriamento Remoto. Natal/RN. Anais do XIV SBSR, 2009.
- Gallo, K.P., McNab, A.L., Karl, T.R., Brown, J.F., Hood, J.J., Tarpley, J.D., 1993. The use of NOAA AVHRR data for assessment of the urban heat island effect. *J Appl Meteorol.* 32 (5), 899–908.
- Gomes, H.B., Ambrizzi, T., Herdies, D.L., Hodges, K., Pontes da Silva, B.F., 2015. Easterly wave disturbances over Northeast Brazil: an observational analysis. *Adv. Meteorol.* 2015.
- Grimmond, S., 2007. Urbanization and global environmental change: local effects of urban warming. *Geogr. J.* 173, 83–88.
- Hansen, A., Cameron, S., Liu, Q., Sun, Y., Weinstein, P., Williams, C., Bi, P., 2015. Transmission of hemorrhagic fever with renal syndrome in China and the role of climate factors: a review. *Int. J. Infect. Dis.* 33, 212–218.
- Hausfather, Z., Menne, M.J., Williams, C.N., Masters, T., Broberg, R., Jones, D., 2013. Quantifying the effect of urbanization on US Historical Climatology Network temperature records. *J. Geophys. Res.* 118 (2), 481–494.
- IBGE, 2016. Arranjos populacionais e concentrações urbanas no Brasil / IBGE, Coordenação de Geografia. - 2. ed. - Rio de Janeiro : IBGE, 2016.e-Book (PDF) – in Portuguese.
- Imhoff, M.L., Zhang, P., Wolfe, R.E., Bounoua, L., 2010. Remote sensing of the urban heat island effect across biomes in the continental USA. *Remote Sens. Environ.* 114 (3), 504–513.
- Inouye, D.W., 2015. The next century of ecology. *Science.* 349 (6248), 565.
- INSTITUTO NACIONAL DE METEOROLOGIA (INMET). Normais Climatológicas do Brasil, 1981–2010. Brasília. 2018.
- Jesen, J.R., 2009. Sensoriamento remoto do ambiente: uma perspectiva em recursos terrestres.[Sl]: Jonh R. Jensen: tradução José Carlos Neves Epiphanio (Coord.)- São José dos Campos, Parêntese.
- Johansen, I.C., 2014. Urbanização e saúde da população: o caso da dengue em Caraguatatuba (SP). Dissertação (Mestrado). Programa de Pós-graduação em Demografia, Instituto de Filosofia e Ciências Humanas, UNICAMP. Campinas-SP (In Portuguese).
- Kazay, D.F., Lucena, A.J., Rotunno Filho, O.C., Peres, L.F., França, J.R.A., 2011. Mudança no uso e cobertura do solo e sua influência na temperatura de superfície: um estudo na região metropolitana do Rio de Janeiro. In: Anais XV Simpósio Brasileiro de Sensoriamento Remoto. INPE, Curitiba, pp. 752–759.
- Kendall, M.G., 1975. Rank Correlation Methods. Griffin, London, UK.
- Kim, Y.H., Baik, J.J., 2002. Maximum urban heat island intensity in Seoul. *J. Appl. Meteorol.* 41 (6), 651–659.
- Kolokotsa, D.D., Giannariakis, G., Gobakis, K., Giannarakis, G., Synnefa, A., Santamouris, M., 2018. Cool roofs and cool pavements application in Acharnes, Greece. *Sustain. Cities Soc.* 37, 466–474.
- Krehbiel, C.P., Jackson, T., Henegry, G.M., 2016. Web-Enabled Landsat Data time series for monitoring urban heat island impacts on land surface phenology. *IEEE Journal of Selected Topics in Applied Earth Observations and Remote Sensing* 9 (5), 2043–2050.
- Kruger, E.L., 2016. Efeitos da ilha de calor nos níveis de conforto em ambientes externos e internos para as condições climáticas de Curitiba. Engenharia Sanitária e Ambiental[online] 21 (3), 459–467 in Portuguese.
- Kruger, E.L., Gonzalez, D.E.G., 2016. Impacts da alteração no albedo das superfícies no microclima e nos níveis de conforto térmico de pedestres em cânions urbanos. Ambiente Construído, Porto Alegre 16 (3), 89–106. Sept.2016 – in Portuguese.
- Laforteza, R., Carrus, G., Sanesi, G., Davies, C., 2009. Benefits and well-being perceived by people visiting green spaces in periods of heat stress. *Urban Forestry & Urban Greening* 8 (2), 97–108.
- Lai, L.W., Cheng, W.L., 2009. Air quality influenced by urban heat island coupled with synoptic weather patterns. *Sci. Total Environ.* 407 (8), 2724–2733.
- Lee, X., Gao, Z., Zhang, C., Chen, F., Hu, Y., Jiang, W., Zeng, Z., 2015. Priorities for boundary layer meteorology research in China. *Bull. Am. Meteorol. Soc.* 96 (9), ES149–ES151.
- Lee, K., Kim, Y., Sung, H.C., Ryu, J., Jeon, S.W., 2020. Trend analysis of urban Heat Island intensity according to urban area change in Asian mega cities. *Sustainability* 12 (1), 112.
- Lemos, J.D.S., 2011. Espacialização da Ilha de Calor do Aglomerado Urbano da Região metropolitana de Curitiba (AU-RMC) em agosto de 2006 a partir da termografia de superfície. In: Anais do XV Simpósio Brasileiro de Sensoriamento Remoto-SBSR. INPE/SELPER, São José dos Campos.
- Li, H., Wolter, M., Wang, X., Sodoudi, S., 2017. Impact of land cover data on the simulation of urban heat island for Berlin using WRF coupled with bulk approach of Noah-LSM. *Theor. Appl. Climatol.* 134 (1–2), 67–81.
- Lombardo, M.A., 1985. Ilha de calor nas metrópoles: o exemplo de São Paulo (Editora Hucitec com apoio de Lalekla SA Comércio e Indústria – in Portuguese).
- Lombardo, M.A., 2009. (2009). Análise das mudanças climáticas nas metrópoles o exemplo de São Paulo e Lisboa. In: CORTEZ, ATC., and ORTIGOZA, SAG., orgs. Da produção ao consumo: impactos socioambientais no espaço urbano [online]. São Paulo: Editora UNESP. São Paulo, Cultura Acadêmica, p. 146.
- Lunardon, K.A.F., 2017. Aspectos do clima urbano de Curitiba/PR: Uma abordagem do campo térmico e sua influência sobre a ocorrência da dengue. Os Desafios da Geografia Física na Fronteira do Conhecimento 1, 2572–2576.
- Macedo Neto, R.X., Ferreira, H.S., Oliveira, T.H., Galvâncio, J.D., Pimentel, R.M.M., 2011. Avaliação dos parâmetros biofísicos da vegetação de caatinga e agricultura irrigada do município de Petrolina – PE através do NDVI, NDWI e temperatura da superfície. (2011) In: SIMPOSIO BRASILEIRO DE SENSORIAMENTO REMOTO, 15. Anais São José dos Campos. INPE 1843–1850.
- Mann, H.B., 1945. Nonparametric Tests against Trend. *Econometrica: Journal of the Econometric Society* 245–259.
- Marengo, J., 2003. Condições climáticas e recursos hídricos no Norte Brasileiro. In: Tucci, C.E., Braga, B. (Eds.), Clima e Recursos Hídricos no Brasil, Associação Brasileira de Recursos Hídricos FBMC/ANA, 9, pp. 117–161. Porto Alegre, Brasil.
- Martínez Navarro, F., Simón-Soria, F., López-Abente, G., 2004. Valoración del impacto de la ola de calor del verano de 2003 sobre la mortalidad. *Gac. Sanit.* 18 (4), 250–258.
- Mashiki, M.Y., Campos, S., 2013. Geoprocessamento Aplicado Na Influência Do Uso E Ocupação Do Solo Na Temperatura Aparente Da Superfície No Município De Botucatu/Sp. Energia na agricultura 28 (3), 143–149.
- Mastrangelo, A., 2016. El agua no se le niega a nadie: estudio social sobre la prevención del dengue en un barrio de Clorinda, Formosa, nordeste argentino. Cuadernos de Ciencias Sociales, año 2 (2), 1–19.
- McDonnell, M.J., MacGregor-Fors, I., 2016. The ecological future of cities. *Science* 352 (6288), 936–938.
- Mills, G., 2008. Micro-and-mesoscale climatology. *Prog. Phys. Geogr.* 32 (3), 293–301.
- Monteiro, F.F., Silveira, A.L.R.C., 2013. Uso de dados de Sensoriamento Remoto para identificação de ilhas de calor em Teresina-PI. In: Paranoá: cadernos de arquitetura e urbanismo, (7) – in Portuguese.
- Morris, C.J.G., Simmonds, I., Plummer, N., 2001. Quantification of the influences of wind and cloud on the nocturnal urban heat island of a large city. *J. Appl. Meteorol.* 40 (2), 169–182.
- Naccarato, K.P., Pinto Jr., O., Pinto, I.R.C.A., 2003. Evidence of thermal and aerosol effects on the cloud-to-ground lightning density and polarity over large urban areas of Southeastern Brazil. *Geophys. Res. Lett.* 30 (13), 1674. <https://doi.org/10.1029/2003GL017496>.
- NOBRE, C.A., YOUNG, A., 2011. Vulnerabilidades das megaciudades brasileiras às mudanças climáticas: região metropolitana de São Paulo. Relatório Final. São Paulo.
- Oke, T.R., 1982. The energetic basis of the urban heat island. *Q. J. R. Meteorol. Soc.* 108, 1–24.
- Oke, T.R., 1987. Boundary layer climates, 2 ed. Routledge, London.
- Oke, T.R., 1988. The urban energy balance. *Prog. Phys. Geogr.* 12, 471–508.
- Oke, T.R., Zeuner, G., Jauregui, E., 1992. The surface energy balance in Mexico City. *Atmosphere Environment.* 26B, 433–444.
- Paula, M.L.M., 2015. Comparação do Campo Térmico da SUC do Município de Vitoria - ES, Em Relação às Alterações de Uso e Ocupação do Solo Urbano em 1991 e 2011. Universidade Federal do Espírito Santo – in Portuguese, Monografia (Geografia).
- Peng, S., Piao, S., Ciais, P., Friedlingstein, P., Ottle, C., Breon, F., Nan, H., Zhou, L., Myeni, R.B., 2012. Surface Urban Heat Island Across 419 Global Big Cities. *Environmental Science & Technology* 46, 696–703.

- Pimenta, D.N., CUNHA, R. V. de (orgs.), 2015. Dengue: teorias e práticas. Editora Fiocruz, Rio de Janeiro, pp. 75–92 in Portuguese.
- Polizel, J., Geotecnologias e Clima Urbano: aplicação dos recursos de Sensoriamento Remoto e sistema de informação geográficas na cidade de Piracicaba, SP. 2009. 153 f (Doctoral dissertation, Tese (Doutorado)-Faculdade de Filosofia, Letras e Ciencias Humanas, Universidade de São Paulo, SP).
- Pontes da Silva, B.F., 2011. Easterly Waves Contribution for the Eastern Northeast Brazil Precipitation: Mean Synoptic Evolution and Numerical Simulations. Master Dissertation, University of São Paulo (in Portuguese).
- Ribeiro, H., Pesquero, C., Coelho, M., 2016. Clima urbano e saúde: Uma revisão sistematizada da literatura recente. Estudos Avançados 30, 67–82 in Portuguese.
- Rizwan, A.M., Dennis, L.Y.C., Liu, C., 2008. A review on the generation, determination and mitigation of Urban Heat Island. J. Environ. Sci. 20, 120–128.
- Roehl, I., Ninivaggi, D.V., Hutchinson, M.L., Farajollahi, A., 2013. Climate change and range expansion of the Asian tiger mosquito (*Aedes albopictus*) in Northeastern USA: implications for public health practitioners. PLoS One 8 (4), e60874.
- Sachindra, D.A., Ng, A.W.M., Muthukumaran, S., Perera, B.J.C., 2016. Impact of climate change on urban heat island effect and extreme temperatures: a case-study. Q. J. R. Meteorol. Soc. 142 (694), 172–186.
- Santamouris, M., 2013. Using cool pavements as a mitigation strategy to fight urban heat island-a review of the actual developments. Renew. Sustain. Energy Rev. 26, 224–240.
- Santana, N.C., 2014. Investigação de ilhas de calor em Brasília: análise multitemporal com enfoque na cobertura do solo. Revista Brasileira de Geografia Física 7 (6), 1044–1054 in Portuguese.
- Santos, T., 2011. Identificação de ilhas de calor em Recife-PE por meio de sensoriamento remoto e dados meteorológicos de superfície. 90p (Doctoral dissertation, Dissertação (mestrado) Programa de Pós graduação em engenharia agrícola. Universidade Federal Rural de Pernambuco-Recife) – in Portuguese.
- Schwarz, N., Lautenbach, S., Seppelt, R., 2011. Exploring indicators for quantifying surface urban heat islands of European cities with MODIS land surface temperatures. Remote Sensing Environ. 115 (12), 3175–3186.
- Segata, J., 2016. A doença socialista e o mosquito dos pobres. Iluminuras, Porto Alegre 17 (42), 372–389.
- Sena, C.A.P., FRANCA, J.D.A., Peres, L.F., 2014. Estudo da Ilha de Calor na Região Metropolitana do Rio de Janeiro usando dados do MODIS. Anuário do Instituto de Geociências 37 (2), 111–122 in Portuguese.
- Silva, M.T., Silva, R.V., Costa, S.C.E., 2011. Impacts da urbanização na temperatura e no balanço de radiação à superfície no município de Fortaleza-CE com base em imagens especrais do TM/Landsat 5. XV Simpósio Brasileiro de Sensoriamento Remoto, Curitiba-PR, Brasil. Anais... São José dos Campos-SP: INPE, 0917-0924 – in Portuguese.
- Sobstyl, J.M., Emig, T., Qomi, M.A., Ulm, F.J., Pellenq, R.M., 2018. Role of city texture in urban heat islands at nighttime. Phys. Rev. Lett. 120 (10), 108701.
- Sousa, S.B., Ferreira, L.G., 2012. Análise de temperatura de superfície em ambientes urbanos: um estudo por meio de sensoriamento remoto no município de Goiânia, Goiás (2002–2011). Confins [Online] 15, 1–19 in Portuguese.
- Souza, D.O., Alvalá, R.C.S., 2014. Observational evidence of the urban heat island of Manaus City, Brazil. Meteorol. Appl. 21 (2), 186–193.
- Souza, L., Postigo, C.P., Oliveira, A., Nakata, C.M., 2009. Urban heat islands and electrical energy consumption. Int. J. Sustain. Energy 28, 113–121. <https://doi.org/10.1080/14786450802453249>.
- Souza, D.O., Alvalá, R.C.S., Nascimento, M.G., 2016. Urbanization effects on the microclimate of Manaus: a modeling study. Atmos. Res. 167, 237–248.
- Stewart, I.D., 2011. A systematic review and scientific critique of methodology in modern urban heat island literature. Int. J. Climatol. 31 (2), 200–217.
- Stewart, I.D., Oke, T.R., 2012. Local climate zones for urban temperature studies. Bull. Am. Meteorol. Soc. 93 (12), 1879–1900.
- Strahler, A., Muchoney, D., Borak, J., Gao, F., Friedl, M., Gopal, S., Hodges, J., Lambin, E., McIver, D., Moody, A., Schaaf, C., Woodcock, C., 1999. MODIS land cover product, algorithm theoretical basis document (ATBD), version 5.0. Boston, MA: Center for Remote Sensing, Department of Geography. Boston University.
- Su, H., Wood, E.F., McCabe, M.F., SU, Z., 2007. Evaluation of remotely sensed evapotranspiration over the CEOP EOP-1 reference sites. Journal of the Meteorological Society of Japan 85A, 439–459.
- Taha, H., 1997. Urban climates and heat islands: albedo, evapotranspiration, and anthropogenic heat. Energy and Buildings 25 (2), 99–103.
- Takiya, H., 2002. Atlas ambiental do município de São Paulo. Prefeitura do Município de São Paulo, São Paulo (Relatório Final, v. 1).
- Tam, B.Y., Gough, W.A., Mohsin, T., 2015. The impact of urbanization and the urban heat island effect on day to day temperature variation. Urban Clim. 12, 1–10.
- Tan, J., Zheng, Y., Tang, X., Guo, C., Li, L., Song, G., Zhen, X., Yuan, D., Kalkstein, A.J., Wan, Z., 2008. New refinements and validation of the MODIS land-surface temperature emissivity products. Remote Sens. Environ. 112, 59–74.
- Tzoulas, K., Korpela, K., Venn, S., Yli-Pelkonen, V., Kazmierczak, A., Niemela, J., 2007. Promoting ecosystem and human health in urban areas using Green infrastructure: a literature review. Landsc. Urban Plan. 81 (3), 167–178.
- Umezaki, Arissa Sary; RIBEIRO, Flávia Noronha Dutra, 2019. Estudo Numérico da Ilha de Calor Urbana da Região Metropolitana de São Paulo Durante um Verão Quente e Seco. In: Sustentabilidade e Interdisciplinaridade. Blucher, São Paulo, pp. 101–124.
- Victoria, R., Matinelli, L., Moraes, J., Ballester, M., Krusche, A., Pellegrino, G., Almeida, R., Richey, J., 1998. Surface air temperature variations in the Amazon region and its border during this century. J. Clim. 11, 1105–1110.
- Voogt, J.A., Oke, T.R., 2003. Thermal remote sensing of urban climates. Remote Sens. Environ. 86 (3), 370–384.
- Wan, Z., 2014. New refinements and validation of the collection-6 MODIS land-surface temperature/emissivity product. Remote Sens. Environ. 140, 36–45.
- Wan, Z., Zhang, Y., Zhang, Q., Li, Z.-L., 2004. Quality assessment and validation of the MODIS land surface temperature. International Journal Remote Sensing 25, 261–274.
- Weng, Q., Lu, D., Schubring, J., 2004. Estimation of land surface temperature–vegetation abundance relationship for urban heat island studies. Remote Sens. Environ. 89 (4), 467–483. <https://doi.org/10.1016/j.rse.2003.11.005>.
- Werneck, D.R., 2018. Estratégias de mitigação das ilhas de calor urbanas: estudos de casos em áreas comerciais em Brasília - DF. In: Dissertação (Mestrado em Arquitetura e Urbanismo) Faculdade de Arquitetura e Urbanismo. Universidade de Brasília, Brasília – in Portuguese.
- Wienert, U., Kuttler, W., 2005. The dependence of the urban heat island intensity on latitude—a statistical approach. Meteorol. Z. 14 (5), 677–686.
- Wilks, D.S., 2011. Statistical methods in the atmospheric sciences (Vol. 100). Academic Press.
- Wong, N.H., Jusuf, S.K., Syaffi, N.I., Chen, Y.X., Hajadi, N., athyanarayanan, H., 2011. Evaluation of the impact of the surrounding urban morphology on building energy consumption. Sol. Energy 85 (1), 57–71.
- Yang, X., Ruby Leung, L., Zhao, N., Zhao, C., Qian, Y., Hu, K., Chen, B., 2017. Contribution of urbanization to the increase of extreme heat events in an urban agglomeration in East China. Geophys. Res. Lett. 44 (13), 6940–6950.
- Yao, R., Luo, Q., Luo, Z., Jiang, L., Yang, Y., 2015. An integrated study of urban microclimates in Chongqing, China: historical weather data, transverse measurement and numerical simulation. Sustain. Cities Soc. 14, 187–199.
- Yavasli, D.D., 2017. Spatio-temporal trends of urban Heat Island and surface temperature in Izmir, Turkey. American Journal of Remote Sensing 5 (3), 24–29.
- Zhang, P., Imhoff, M.L., Bounoua, L.& Wolfe, R.E., 2012. Exploring the influence of impervious surface density and shape on urban heat islands in the Northeast United States using MODIS and Landsat. Canadian Journal Remote Sensing 38 (4), 441–451.
- Zhao, S., Zhou, D., Liu, S., 2016. Data concurrence is required for estimating urban heat island intensity. Environ. Pollut. 208, 118–124.
- Zhou, Y., Smith, S.J., Zhao, K., Imhoff, M., Thomson, A., Bond-Lamberty, B., Elvidge, C.D., 2015. A global map of urban extent from nightlights. Environ. Res. Lett. 10 (5), 054011.
- Zhou, B., Rybski, D., Kropp, J.P., 2017. The role of city size and urban form in the surface urban heat island. Science Report 7, 4791.